Optical properties and diffraction effects in opal photonic crystals

Alessandra Balestreri and Lucio Claudio Andreani
Dipartimento di Fisica "Alessandro Volta," Università degli Studi di Pavia, via Bassi 6, I-27100 Pavia, Italy

Mario Agio*
Dipartimento di Fisica "Alessandro Volta," Università degli Studi di Pavia, via Bassi 6, I-27100 Pavia, Italy
(Received 27 May 2006; published 6 September 2006)

Optical properties of fcc opals oriented along the [111] direction are calculated by means of a scattering-matrix approach based on approximating each sphere with cylindrical slices. The use of a plane-wave basis in each layer allows distinguishing zero-order reflection and transmission from higher-order (diffraction) spectra. Optical spectra at large values of the angle of incidence indicate the presence of diffraction effects and of polarization mixing along the *LW* orientation. Reflectance and transmittance in the high-energy region show a rich spectral dependence and compare reasonably well with recent experimental observations on polystyrene opals. Diffraction spectra as a function of the number of layers display an oscillatory behavior, pointing to the existence of a Pendellösung phenomenon, related to the exchange of energy between two propagating modes in the investigated three-dimensional photonic crystal. This phenomenon could be observed in transmittance experiments on high-quality opals with controlled thickness.

DOI: 10.1103/PhysRevE.74.036603 PACS number(s): 42.70.Qs, 41.20.Jb, 78.20.Bh, 78.40.−q

I. INTRODUCTION

Since the first proposal in 1987 [1,2], there has been growing interest towards photonic crystals (PhCs) in view of the possibility to control light propagation in all spatial directions [3–8]. Among all investigated structures, artificial opals are readily available three-dimensional (3D) PhCs. They consist of dielectric spheres (usually made of polystyrene or silica) arranged in a close-packed fcc lattice oriented along the [111] crystallographic direction. Bare opals can be produced with bottom up approaches based on casting from colloidal solutions, possibly followed by infiltration with high-index materials and template removal in order to obtain inverse opals [9–12].

The optical properties of opals have been subject to a number of investigations and are increasingly well known over the years [13–43]. Superprism effects [18,32], superluminality [21,24,42,43], diffraction phenomena [14,25,28,29,37,40] and the control of spontaneous emission [20,30,35] are just a few of the interesting issues to be studied in opal structures. While most previous works were concerned with the fundamental stop band (or Bragg peak) and its evolution as a function of incidence angle, with multiple peaks related to diffraction appearing at high angles [28,29,31,36,41], recent studies on high-quality opals with large single domains allowed a precise determination of optical spectra in the region around and above the second-order stop band [12,38,39], where diffraction effects due to higher-order crystalline planes come into play even at normal incidence. These developments call for theories of the optical response of opals which reproduce the main phenomena associated with diffraction, with a good compromise between accuracy and computational effort.

In this work we give a systematic study of optical properties of fcc opals, focusing in particular on optical spectra at large incidence angles and/or in the high-energy region where diffraction effects play a crucial role. To this purpose we adopt a scattering-matrix or Fourier-modal method which has been developed in order to treat patterned multilayer structures [44–47]: the approach applies to a stack of layers, each of which is periodic in the two-dimensional (2D) plane and is homogeneous in the vertical (z) direction. In order to employ this method, which is a numerically convenient one and includes diffraction effects in a natural way, we subdivide each sphere of the fcc structure into a set of cylinders oriented along the [111] direction and optimize their dimensions in order that the band structure in the energy region of interest is well reproduced.

While the photonic band structure of direct and inverse opals is well known from a variety of methods [48–50], the simplest one being 3D plane-wave expansion [3,51], the optical properties (i.e., reflection, transmission, and diffraction) are much more difficult to calculate. Other methods which have been applied to a study of optical properties of opals are now briefly discussed. First, a scalar-wave approximation [42,52–54] is frequently employed for a quick analysis of experimental results in the region of the first-order stop band. This approximation is basically one dimensional and is clearly unsuitable to study diffraction effects. Second, the finite-difference time domain (FDTD) method has been applied to study light propagation in 3D photonic crystals [55], however it requires heavy numerical calculations, especially for thick samples. Third, the transfer matrix method [56] has been used in order to study the optical properties of opals in the surroundings of the first pseudogap [22,31,57]. This method presents some difficulties when dealing with thick samples. Fourth, the vectorial Korringa-Kohn-Rostoker (KKR) method is an accurate one for treating spherical particles in colloidal solutions [58–61]. The method relies on a subdivision of the 3D structure in 2D layers of spheres and it

*Present address: Laboratory of Physical Chemistry, ETH Zurich, CH-8093 Zurich, Switzerland.

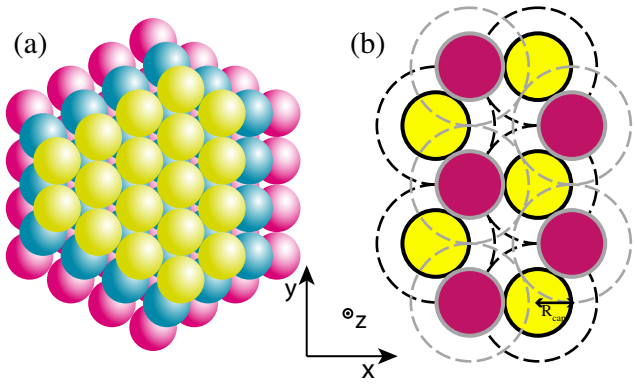

FIG. 1. (Color online) Top view of the opaline structure: (a) Three consecutive layers arranged in the *ABC* order along the [111] direction. (b) Cross section of the spheres of two consecutive layers: dashed, maximal cross section in each layer; full lines, cross section at the contact point between spheres of the interpenetrating layers with the definition of the cap radius R_{cap}.

is hard to apply to close-packed opals, in which two consecutive layers along the (111) direction partially overlap. None of these methods has been applied to a study of diffraction spectra, as done in the present work.

The rest of this paper is organized as follows. In Sec. II we give a description of the opal structure as represented in this work, and we compare the photonic band dispersion of the actual opaline structure with that obtained by replacing each sphere with a set of cylinders. In Sec. III we present results for optical spectra in the low-energy region for different incidence angles, discussing also diffraction spectra and the effects of polarization mixing along the *LW* orientation. In Sec. IV we analyze optical spectra at normal incidence in the high-energy region, focusing in particular on diffraction phenomena and on their dependence on the number of layers: we verify and quantitatively evaluate the phenomenon of "Pendellösung" oscillations, which is well known in X-ray diffraction [62] and has been recently predicted for 2D photonic crystals [63]. Section V contains a brief summary and discussion of the main results.

II. THEORETICAL METHOD

A. Structure description and scattering-matrix approach

A direct opal is constituted of dielectric spheres arranged in a close-packed fcc lattice. As it can be seen from Fig. 1(a), which shows a top view along the [111] direction, the opal structure can also be described as a close-packed lattice where each layer of spheres is shifted in the x direction with respect to the previous one, i.e., with a stacking sequence *ABC*, *ABC*, etc. Two consecutive layers are interpenetrating. Notice that the spheres in each layer are arranged in a triangular lattice of periodicity $d=a/\sqrt{2}$, where a is the lattice constant of the fcc lattice, while the cross sections of the spheres in two consecutive layers at the contact point form a graphite lattice, as seen in Fig. 1(b).

A vertical cross section of the opal structure in the xz plane is shown in Fig. 2(a), where the contact points between

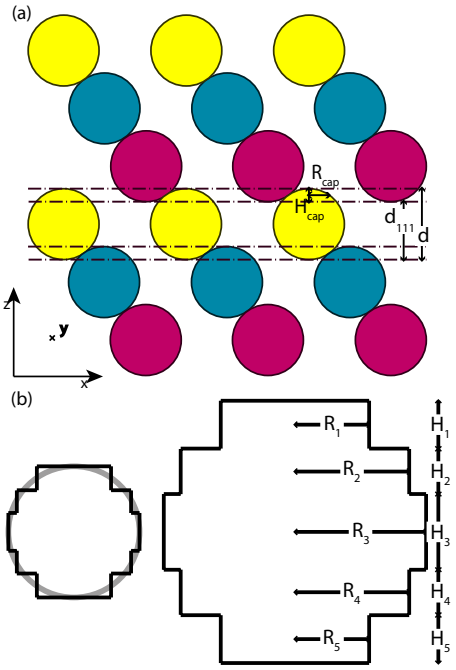

FIG. 2. (Color online) Front view of the opaline structure (a) and of a single sphere subdivided in five cylinders (b). Sphere diameter d, distance between two consecutive layers d_{111}, cap height H_{cap} and radius R_{cap} are shown in (a).

two interpenetrating layers can also be seen. The distance d_{111} between two consecutive layers along the [111] direction is smaller than the sphere diameter d and is given by

$$d_{111} = \sqrt{\frac{2}{3}}d. \quad (1)$$

Each layer is shifted in the x direction by $d/\sqrt{3}$ with respect to the previous one. Notice that the vertical stacking of the 2D planes is similar to the layered dielectric structure described in Refs. [5,64,65].

In this work we calculate the optical spectra of the opal structure by using the scattering-matrix method according to the procedure of Whittaker and Culshaw [47]. Through this approach one can treat a structure constituted by multiple layers, each of which is patterned in the xy plane but is homogeneous in the z direction. The electromagnetic field in each layer is represented in a Fourier or plane-wave basis. The idea of the present work is to use the method by approximating each sphere with a set of cylinders, whose axes are oriented along the [111] direction. In particular we obtain satisfactory results by subdividing each sphere into five cylinders, as it is shown in Fig. 2(b), where the relevant dimensions (cylinder radii and heights) are defined. An important feature of this approach is to mimic the interpenetration of two consecutive layers along the [111] direction: this is obtained by making the outermost cylinders (numbers 1 and 5) to be of the same height $H_{cap}=(1-\sqrt{2/3})d$ as the overlapping layers, see Fig. 2(a). Those cylinders are arranged in a graphite lattice shifted by $R_{cap}=d/(2\sqrt{3})$ with respect to the previous layer [see Fig. 1(b)], while the three inner cylinders (2–4) are arranged according to the usual triangular lattice in their respective planes. This way, each layer of the model

structure is homogeneous along the z direction and it has the same 2D Bravais lattice (albeit with a different unit cell basis), thereby allowing to apply the scattering-matrix approach in a plane-wave basis. This approach is very convenient as it allows distinguishing zero-order Bragg reflection and transmission from higher-order processes: the latter ones correspond to diffraction in directions other than those of the transmitted and reflected beams.

B. Band structure comparison

The photonic band structure is obtained starting from the second-order wave equation for the magnetic field

$$\nabla \times \left(\frac{1}{\varepsilon(r)} \nabla \times \mathbf{H} \right) = \frac{\omega^2}{c^2} \mathbf{H}. \tag{2}$$

By using the plane-wave expansion technique, we transform Eq. (2) into an eigenvalue problem and we calculate the inverse dielectric matrix following the procedure of Ho, Chan, and Soukoulis [51]. This method allows us to calculate the photonic bands for an infinite crystal, for either the fcc structure constituted by spheres or when each sphere is subdivided into a set of cylinders. A comparison between the two band structures is a crucial test of the accuracy of the approach.

In the present work we limit our study to bare opals made of polystyrene spheres (refractive index $n_{\text{poly}}=1.58$) in air ($n_{\text{air}}=1$). We have optimized the cylinder parameters in order to reproduce the actual band structure of the opal with spheres in a range of dimensionless frequencies up to $\omega a/(2\pi c) \leqslant 2$. The following conditions are imposed: (i) cylinders 1 and 5 are equal, cylinders 2 and 4 are equal; (ii) the height of cylinders numbers 1 and 5 is equal to the height H_{cap} of the sphere caps in the overlapping layers and their radius equals the radius R_{cap} of the sphere cross sections at the contact point (see Fig. 2); (iii) the total height of a layer of cylinders 1–5 is equal to the sphere diameter d; (iv) the total dielectric filling fraction is fixed to that of the spheres, i.e., $f=\pi/(3\sqrt{2})=0.7405$. We have seen that the best choice for the cylinder parameters is as follows:

$$H_1 = H_5 = 0.1835d, \quad R_1 = R_5 = 0.2886d,$$

$$H_2 = H_4 = 0.1721d, \quad R_2 = R_4 = 0.4309d,$$

$$H_3 = 0.2888d, \quad R_3 = 0.5000d. \tag{3}$$

The radius of cylinder number 3 turns out to be the same as the radius of the sphere. It should be noticed that condition (iii) for the total layer height is essential in order to give a good representation of light coupling at the interfaces for an opal of finite size.

In Fig. 3 the calculated photonic band dispersion for the fcc structure with both spheres and cylinders is shown. The agreement of the photonic bands is amazingly good, even in the high-energy region (where the folding of free-photon bands corresponds to the occurrence of diffraction) and also along directions different from ΓL, i.e., for non-normal incidence. In the following, all the optical spectra are calculated for the structure made of cylinders. For the sake of consistency we compare these spectra with the band structure calculated for an infinite crystal with the same five-cylinder approximation.

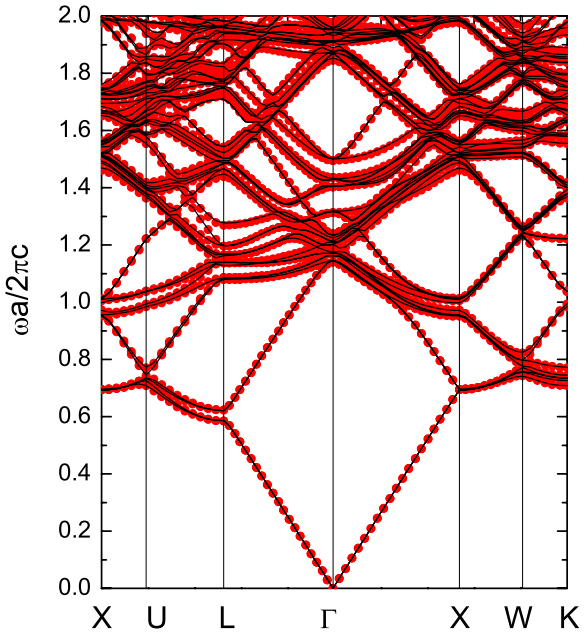

FIG. 3. (Color online) Band structure of an fcc lattice made of polystyrene ($n=1.58$) spheres in air (dots) and of the same lattice where each sphere is subdivided into five cylinders with optimized dimensions given in the text (solid line).

III. OPTICAL PROPERTIES IN THE LOW-ENERGY REGION

We calculate the optical spectra in the low-energy region for a polystyrene opal constituted by 21 layers (i.e., by seven periods along the [111] direction). In Fig. 4 we compare the photonic band structure along the ΓL and LW directions in the first Brillouin zone with zero-order reflectance (R) and transmittance (T), as well as diffraction (D) spectra calculated as

$$D = 1 - R - T. \tag{4}$$

The quantity D represents the intensity of light diffracted in all directions, except those of the reflected and transmitted beams, as previously mentioned in Sec. II A. The spectra are calculated for transverse magnetic (TM) and transverse electric (TE) polarizations of the incident beam and are taken for an incidence angle in air that increases from 0 to 70 degrees in steps of 5 degrees. All the curves are convoluted with a Gaussian line shape of variance $\sigma a/(2\pi c)=0.005$ in order to approach experimental conditions in which some broadening is inevitably present. We can clearly see the Bragg peak and its frequency dispersion for different incidence angles, in close agreement with the band structure, for both TM and TE incident light. In the same figure we can also notice a peak in reflection that crosses the pseudogap for incidence angles greater than 50 degrees: this feature arises from band cou-

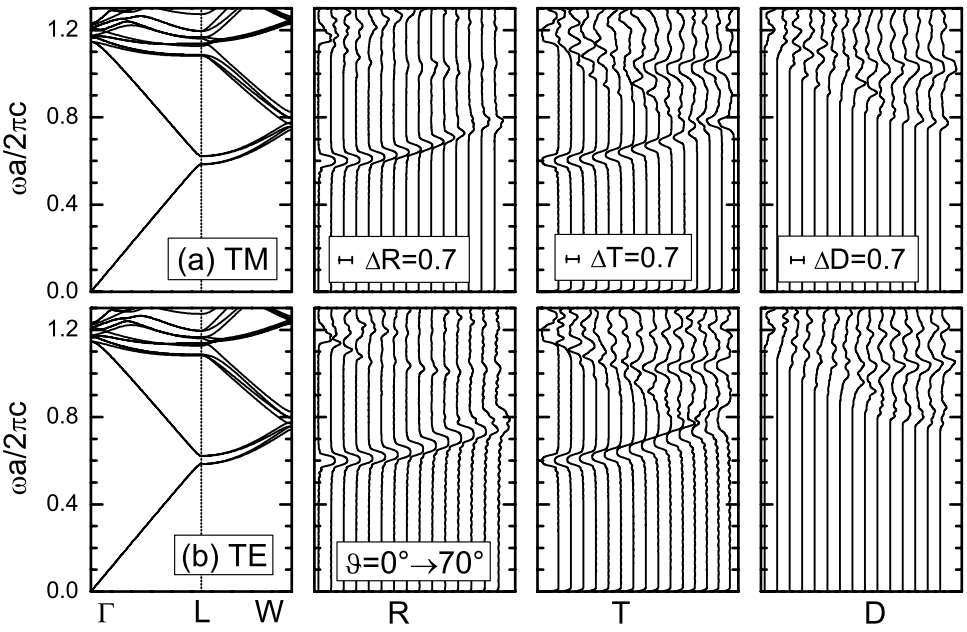

FIG. 4. Band structure along LW and optical spectra at finite incidence angle in the ΓLW plane for a polystyrene opal made of 21 layers: incident light has (a) TM polarization and (b) TE polarization. The incidence angle θ in air increases in steps of 5 degrees. The spectra are convoluted with a Gaussian line shape of variance $\sigma a/(2\pi c)=0.005$ and are shifted for clarity.

pling occurring near the W point of the Brillouin zone, related to multiple diffraction from {111} and {200} Bragg planes, as previously observed and discussed [28,29,31,36,41]. This is confirmed by examination of the diffraction spectra. Between $\omega a/(2\pi c)=1.0$ and 1.2 we can see many diffraction structures, related to the flat bands in that energy region. These structures are more visible in transmittance than in reflectance: this happens because the diffracted beam subtracts intensity both to the transmitted and reflected beams, but the effect of R spectra is a minor one since reflectance is small anyway.

It must be noticed that the labels TE and TM can be referred only to the incident light beam: in fact, since the ΓLW plane is not a symmetry plane of the fcc structure, there is a mixing between the two polarizations for the outgoing light. In Fig. 5 the intensity of TM-polarized outgoing light for TE incoming light in transmission and reflection is shown. The incidence angles are the same as in the previous figure and all the curves are convoluted with the same Gaussian line shape. It can be noticed that there is no mixing at normal incidence, in agreement with group-theoretical considerations in the presence of a three fold rotation axis. The TE-TM mixing is greater in transmittance than in reflectance and it grows considerably in the same range of angles and energies for which the diffracted intensity becomes appreciable: thus, polarization mixing and diffraction are related to each other. It would be interesting to verify these predictions by polarization-resolved transmission measurements.

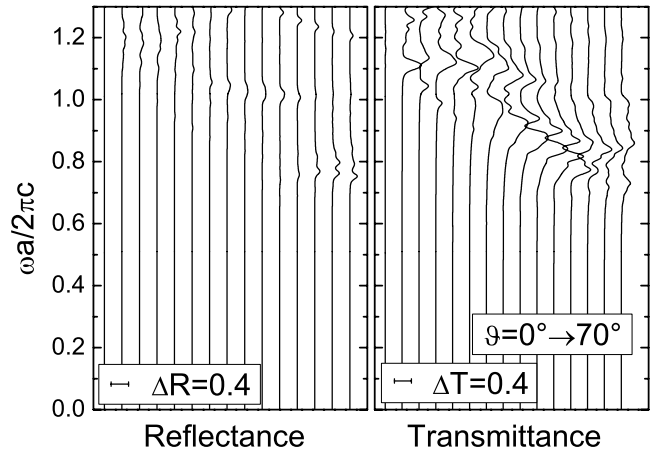

FIG. 5. Mixing TE-TM, or TM-polarized outgoing light for TE-polarized incoming light, for a polystyrene opal made of 21 layers. The incidence angle θ increases in steps of 5 degrees.

The phase delay of the transmitted beam can also be obtained by the scattering matrix method. Comparison with interferometric measurements of phase delay and group velocity on high-quality polystyrene opals is reported in Ref. [43], showing very good agreement between experiment and theory. Therefore, phase results will not be discussed in the present paper.

IV. OPTICAL SPECTRA IN THE HIGH-ENERGY REGION

In this section we study the optical response of an opaline structure in the high-energy region, around and above the frequencies of the second-order stop band. The comparison of the photonic bands in Fig. 3 guarantees that the cylinder approximation of the spheres remains quantitatively adequate. We focus on optical spectra at normal incidence, i.e., along the ΓL direction. Since the incident field belongs to the twofold-degenerate irreducible representation of the C_{3v} group (which is the small point group along ΓL), there is no distinction between TM and TE polarized light and all polarizations in the (111) plane are equivalent [66].

A. Optical properties along ΓL

In Fig. 6 we compare reflectance (R), transmittance (T) and diffraction (D) spectra of a 21-layers opal with the photonic band structure, calculated along ΓL line for the infinite crystal with the five-cylinders approximation. As in the pre-

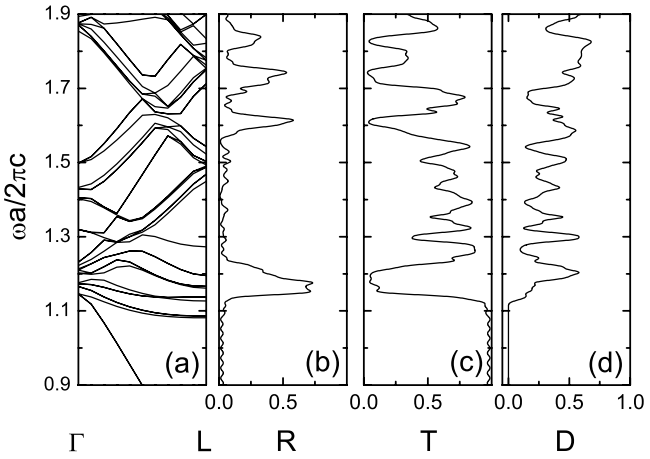

FIG. 6. (a) Band structure along ΓL for an infinite polystyrene opal in the five-cylinders approximation, (b) reflectance, (c) transmittance, (d) diffraction spectra at normal incidence for a polystyrene opal made of 21 layers.

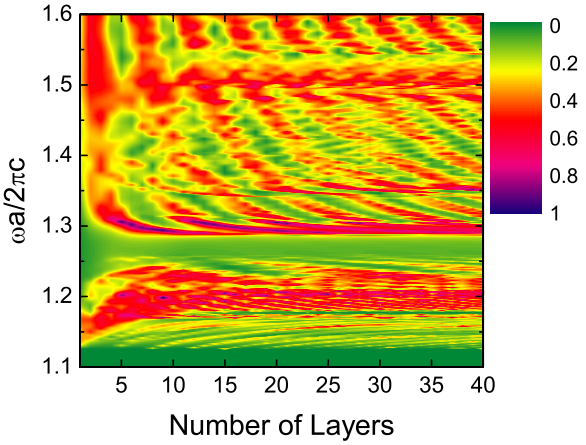

FIG. 7. (Color online) Diffraction intensity in the high-energy region for a polystyrene opal as a function of frequency and number of layers.

ceding section, optical spectra are convoluted with a Gaussian line shape of variance $\sigma a/(2\pi c)=0.005$.

The first peak in reflection, at $\omega a/(2\pi c)=1.15$, corresponds to a dip in transmission and to a region in which the free-photon-like bands split at the center of the Brillouin zone. This second-order pseudogap, unlike the first pseudogap, is filled with low-dispersion bands arising from the folding of plane waves with reciprocal lattice vectors different from (000) and (111). In other words, these bands are associated with diffraction processes in directions other than forward- or backward propagation. This interpretation is confirmed by diffraction spectra in Fig. 6(d), in which the onset of diffraction at $\omega a/(2\pi c)=1.1$ and a pronounced peak at $\omega a/(2\pi c)=1.2$ are clearly visible.

The structures between $\omega a/(2\pi c)=1.2$ and 1.6, also visible in transmission spectra, are due again to diffraction by higher-order Bragg planes. In this frequency interval there are many photonic bands with different dispersion, so assigning each peak in diffraction intensity to a specific band becomes quite difficult. Notice, however, that diffraction features can be recognized in transmission spectra even when the reflected intensity is very small. The diffraction intensity in this frequency region as a function of sample thickness will be dealt with in the next section.

At higher energies there are three other peaks in reflection. The first one [at $\omega a/(2\pi c)=1.61$] is due to an anticrossing in the free-photon bands at about $k=0.7\sqrt{3}\pi/a$, while the second one [at $\omega a/(2\pi c)=1.74$] is due to a splitting at the L point and is related to the third-order stop band. Both of them correspond to dips in transmission and in diffraction. The third peak [at $\omega a/(2\pi c)=1.84$] corresponds to a dip in transmission and falls in a broad shoulder of the diffraction spectrum: like the first peak, it is related to an anticrossing of free-photon levels close to the L point of the Brillouin zone.

We now compare our theoretical results with the experimental reflectance and transmittance spectra reported in Fig. 4 of Ref. [38]. The experimental R spectrum is characterized by two pronounced structures between dimensionless frequencies 1.1 and 1.2, followed by a flat background and two other peaks at $\omega a/(2\pi c)=1.6$ and $\omega a/(2\pi c)=1.72$. These features are qualitatively reproduced by our calculation, except for the fact that we get a narrower reflectivity peak in correspondence with the second-order stop band. The minima in the experimental transmittance spectrum are fairly well reproduced. The remaining discrepancies are attributed to the effects of imperfections and resulting diffusion, which may be particularly severe within the second-order stop band where several low-dispersion bands are present.

B. Pendellösung effect

We studied the dependence of diffraction intensity as a function of sample thickness, i.e., of the layer number N. In Fig. 7 the diffraction intensity in the high-energy region is shown in the form of a contour plot for N ranging from 1 to 40. Nearly periodic oscillations can be noticed at specific frequencies and the oscillation period is also a function of frequency. The periodic behavior is evidence of a mutual exchange of energy between two or more beams inside the crystals. This effect is analogous to the well known "Pendellösung" phenomenon, that has been extensively studied for X-ray or neutron diffraction in ordinary crystals [62]. The same phenomenon has been recently studied in 2D photonic crystals [63] as an effect related to negative refraction. Figure 7 shows that the Pendellösung effect is also present for 3D photonic crystals in the energy region above the diffraction cutoff.

In order to appreciate the oscillatory behavior more clearly, we plot in Fig. 8 the diffracted intensity as a function of N for dimensionless frequencies $\omega a/(2\pi c)=1.33$ and 1.30. Considering N as a continuous variable, the period of oscillations is close to $\Delta N=6.6$ for Fig. 8(a) and $\Delta N=8.7$ for Fig. 8(b). Furthermore, it can be noticed that the Pendellösung oscillations for $\omega a/(2\pi c)=1.30$ are damped. It is interesting to relate these features to the photonic band structure. Figure 9 shows the photonic bands that are allowed or forbidden for light coupling, due to symmetry reasons [67]. Only coupled bands are responsible for light propagation and

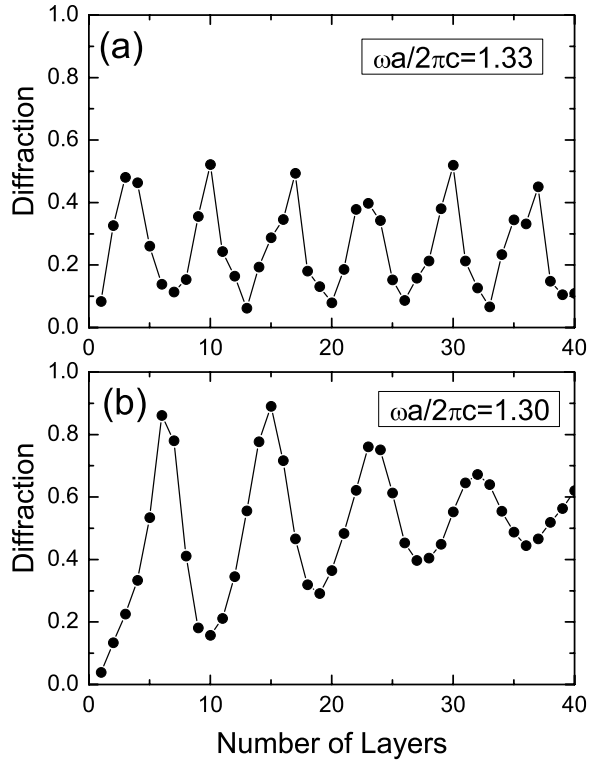

FIG. 8. Diffraction intensity as a function of the number of layers for two different frequencies: (a) $\omega a/(2\pi c)=1.33$ and (b) $\omega a/(2\pi c)=1.30$.

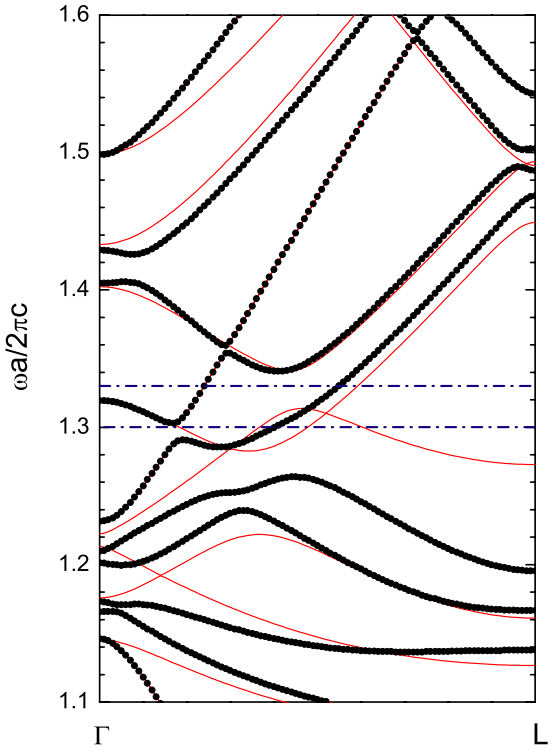

FIG. 9. (Color online) Photonic band structure along ΓL. Dots, bands that couple to incident light and are responsible for periodicity of the diffracted intensity; thin solid lines, uncoupled bands. The horizontal dashed-dotted lines indicate the frequencies of Fig. 8.

for diffraction effects along this specific direction. In order to give a quantitative description of the Pendellösung phenomenon, we notice that for $\omega a/(2\pi c)=1.33$ and $\omega a/(2\pi c)=1.30$ only two photonic modes are allowed in the crystal. In this case the period Λ_{Pend} of the oscillation of the diffraction intensity is inversely proportional to the difference between the two relevant wave vectors,

$$\Lambda_{\mathrm{Pend}}=\frac{2\pi}{\Delta k}, \tag{5}$$

where $\Delta k=k_2-k_1$. For the case of Fig. 8(a), $\omega a/(2\pi c)=1.33$, we get $\Delta k=0.31\cdot\sqrt{3}\pi/a=0.97d_{111}$ which gives $\Lambda_{\mathrm{Pend}}=6.5d_{111}$, in agreement with the above value of ΔN. For the case of Fig. 8(b), $\omega a/(2\pi c)=1.30$, we get $\Delta k=0.24\cdot\sqrt{3}\pi/a=0.75d_{111}$, whence $\Lambda_{\mathrm{Pend}}=8.4d_{111}$ which also agrees with the period ΔN determined from the figure. Thus we conclude that the Pendellösung oscillations originate from spatial beatings between the fundamental propagating mode along the [111] direction and a diffracted mode. These oscillations are visible in transmittance spectra as well. It would be interesting to verify these predictions experimentally on high-quality opals with controlled thickness.

It is interesting to notice that the frequency $\omega a/(2\pi c)=1.30$ is slightly below a minimum of the allowed mode at $k=0.17\sqrt{3}\pi/a$ in Fig. 9. Thus a single mode at $k=0.17\sqrt{3}\pi/a$ is excited, but with a small imaginary part of the wave vector, leading to a damping of the Pendellösung oscillations as observed in Fig. 8(b). Also, when more than two wave vectors are allowed for light coupling the situation is much more complicated. In this case the exchange of energy is among three or more states and it may not result in periodic oscillations when the beating periods are incommensurate. Examples of this situation can also be recognized in Fig. 7.

V. CONCLUSIONS

The scattering-matrix method is seen to be a powerful approach for calculating the optical response of opal photonic crystals, provided the spheres in the fcc structure are approximated with cylindrical layers. It is important to take into account the caps of the spheres in the overlapping layers in order to obtain a good representation of the photonic bands in the region where diffraction effects become relevant. Reflectance and transmittance at large values of the angle of incidence are characterized by the presence of spectral features related to diffraction: this interpretation is confirmed by the explicit calculation of diffracttion spectra. Polarization mixing effects along the LW orientation are predicted and are particularly evident in the calculated transmittance. Optical spectra at normal incidence in the high-energy region present several interesting features that correspond reasonably well to recent experimental results on polystyrene opals [38]: remaining differences point to the role of diffusion related to disorder in the samples, especially in the vicinity of the second-order stop band. Finally, periodic oscillations in the diffracted (and also in the transmit-

ted) intensity indicate the occurrence of a Pendellösung phenomenon, as recently predicted for 2D photonic crystals [63] and in analogy with X-ray diffraction in ordinary crystals. These results are examples of the richness of physical phenomena related to light propagation in 3D photonic crystals and are amenable to experimental verification in polystyrene or silica opals.

ACKNOWLEDGMENTS

The authors are grateful to J. Galisteo-López and C. López for many helpful conversations. This work was supported by MIUR through Cofin 2004 program and through FIRB project "Miniaturized electronic and photonic systems."

[1] E. Yablonovitch, Phys. Rev. Lett. **58**, 2059 (1987).
[2] S. John, Phys. Rev. Lett. **58**, 2486 (1987).
[3] J. D. Joannopoulos, R. D. Meade, and J. N. Winn, *Photonic Crystals* (Princeton University Press, Princeton, NJ, 1995).
[4] K. Sakoda, *Optical Properties of Photonic Crystals* (Springer-Verlag, New York, 2001).
[5] S. G. Johnson and J. D. Joannopoulos, *Photonic Crystals: The Road from Theory to Practice* (Kluwer, Boston, 2002).
[6] *Photonic Crystals: Physics, Fabrication and Applications*, edited by K. Inoue and K. Ohtaka (Springer-Verlag, New York, 2004).
[7] *Photonic Crystals: Advances in Design, Fabrication, and Characterization*, edited by K. Busch, S. Lölkes, R. B. Wehrspohn, and H. Föll (Wiley-VCH, Weinheim, 2004).
[8] J.-M. Lourtioz, H. Benisty, V. Berger, J.-M. Gérard, D. Maystre, and A. Tchelnokov, *Photonic Crystals: Towards Nanoscale Photonic Devices* (Springer-Verlag, Berlin, 2005).
[9] J. E. G. J. Wijnhoven and W. L. Vos, Science **281**, 802 (1998).
[10] A. A. Zakhidov, R. H. Baughman, Z. Iqbal, C. Cui, I. Khayrullin, S. O. Dantas, J. I. Marti, and V. G. Ralchenko, Science **282**, 897 (1998).
[11] A. Blanco, E. Chomski, S. Grabtchak, M. Ibisate, S. John, S. W. Leonard, C. López, F. Meseguer, H. Miguez, J. P. Mondia, G. A. Ozin, O. Toader, and H. M. van Driel, Nature (London) **405**, 437 (2000).
[12] Yu. A. Vlasov, X. Z. Bo, J. C. Sturm, and D. J. Norris, Nature (London) **414**, 289 (2001).
[13] W. L. Vos, R. Sprik, A. van Blaaderen, A. Imhof, A. Lagendijk, and G. H. Wegdam, Phys. Rev. B **53**, 16231 (1996).
[14] I. I. Tarhan and G. H. Watson, Phys. Rev. Lett. **76**, 315 (1996).
[15] V. N. Bogomolov, S. V. Gaponenko, I. N. Germanenko, A. M. Kapitonov, E. P. Petrov, N. V. Gaponenko, A. V. Prokofiev, A. N. Ponyavina, N. I. Silvanovich, and S. M. Samoilovich, Phys. Rev. E **55**, 7619 (1997).
[16] Yu. A. Vlasov, V. N. Astratov, O. Z. Karimov, A. A. Kaplyanskii, V. N. Bogomolov, and A. V. Prokofiev, Phys. Rev. B **55**, R13357 (1997).
[17] H. Míguez, C. López, F. Meseguer, A. Blanco, L. Vázquez, R. Mayoral, M. Ocaña, V. Fornés, and A. Mifsud, Appl. Phys. Lett. **71**, 1148 (1997).
[18] H. Kosaka, T. Kawashima, A. Tomita, M. Notomi, T. Tamamura, T. Sato, and S. Kawakami, Phys. Rev. B **58**, R10096 (1998).
[19] H. Míguez, A. Blanco, F. Meseguer, C. López, H. M. Yates, M. E. Pemble, V. Fornés, and A. Mifsud, Phys. Rev. B **59**, 1563 (1999).
[20] M. Megens, J. E. G. J. Wijnhoven, A. Lagendijk, and W. L. Vos, Phys. Rev. A **59**, 4727 (1999).
[21] Y. A. Vlasov, S. Petit, G. Klein, B. Honerlage, and C. Hirlimann, Phys. Rev. E **60**, 1030 (1999).
[22] A. Reynolds, F. López-Tejeira, D. Cassagne, F. J. García-Vidal, C. Jouanin, and J. Sánchez-Dehesa, Phys. Rev. B **60**, 11422 (1999).
[23] M. S. Thijssen, R. Sprik, J. E. G. J. Wijnhoven, M. Megens, T. Narayanan, A. Lagendijk, and W. L. Vos, Phys. Rev. Lett. **83**, 2730 (1999).
[24] A. Imhof, W. L. Vos, R. Sprik, and A. Lagendijk, Phys. Rev. Lett. **83**, 2942 (1999).
[25] R. M. Amos, J. G. Rarity, P. R. Tapster, T. J. Shepherd, and S. C. Kitson, Phys. Rev. E **61**, 2929 (2000).
[26] Yu. A. Vlasov, V. N. Astratov, A. V. Baryshev, A. A. Kaplyanskii, O. Z. Karimov, and M. F. Limonov, Phys. Rev. E **61**, 5784 (2000).
[27] Z. Y. Li and Z. Q. Zhang, Phys. Rev. B **62**, 1516 (2000).
[28] H. M. van Driel and W. L. Vos, Phys. Rev. B **62**, 9872 (2000).
[29] W. L. Vos and H. M. van Driel, Phys. Lett. A **272**, 101 (2000).
[30] H. P. Schriemer, H. M. van Driel, A. F. Koenderink, and W. L. Vos, Phys. Rev. A **63**, 011801(R) (2000).
[31] S. G. Romanov, T. Maka, C. M. Sotomayor Torres, M. Müller, R. Zentel, D. Cassagne, J. Manzanares-Martinez, and C. Jouanin, Phys. Rev. E **63**, 056603 (2001).
[32] T. Ochiai and J. Sánchez-Dehesa, Phys. Rev. B **64**, 245113 (2001).
[33] J. F. Galisteo López and W. L. Vos, Phys. Rev. E **66**, 036616 (2002).
[34] V. N. Astratov, A. M. Adawi, S. Fricker, M. S. Skolnick, D. M. Whittaker, and P. N. Pusey, Phys. Rev. B **66**, 165215 (2002).
[35] A. F. Koenderink, L. Bechger, H. P. Schriemer, A. Lagendijk, and W. L. Vos, Phys. Rev. Lett. **88**, 143903 (2002).
[36] J. F. Galisteo-López, E. Palacios-Lidón, E. Castillo-Martínez, and C. López, Phys. Rev. B **68**, 115109 (2003).
[37] L. M. Goldenberg, J. Wagner, J. Stumpe, B.-R. Paulke, and E. Görnitz, Physica E (Amsterdam) **17**, 433 (2003).
[38] J. F. Galisteo-López and C. López, Phys. Rev. B **70**, 035108 (2004).
[39] H. Míguez, V. Kitaev, and G. A. Ozin, Appl. Phys. Lett. **84**, 1239 (2004).
[40] F. García-Santamaría, J. F. Galisteo-López, P. V. Braun, and C. López.Phys. Rev. B **71**, 195112 (2005).
[41] E. Pavarini, L. C. Andreani, C. Soci, M. Galli, F. Marabelli, and D. Comoretto, Phys. Rev. B **72**, 045102 (2005).
[42] G. von Freymann, S. John, S. Wong, V. Kitaev, and G. A. Ozin, Appl. Phys. Lett. **86**, 53108 (2005).
[43] J. F. Galisteo-López, M. Galli, M. Patrini, A. Balestreri, L. C. Andreani, and C. López, Phys. Rev. B **73**, 125103 (2006).
[44] E. Popov, Prog. Opt. **31**, 141 (1993).

[45] Ph. Lalanne and G. M. Morris, J. Opt. Soc. Am. A **13**, 779 (1996).
[46] S. Peng and G. M. Morris, J. Opt. Soc. Am. A **13**, 993 (1996).
[47] D. M. Whittaker and I. S. Culshaw, Phys. Rev. B **60**, 2610 (1999).
[48] H. S. Sözüer, J. W. Haus, and R. Inguva, Phys. Rev. B **45**, 13962 (1992).
[49] K. Busch and S. John, Phys. Rev. E **58**, 3896 (1998).
[50] A. Moroz and C. Sommers, J. Phys.: Condens. Matter **11**, 997 (1999).
[51] K. M. Ho, C. T. Chan, and C. M. Soukoulis, Phys. Rev. Lett. **65**, 3152 (1990).
[52] K. W.-K. Shung and Y. C. Tsai, Phys. Rev. B **48**, 11265 (1993).
[53] D. M. Mittleman, J. F. Bertone, P. Jiang, K. S. Hwang, and V. L. Colvin, J. Chem. Phys. **111**, 345 (1999).
[54] A. Mihi, H. Míguez, I. Rodríguez, S. Rubio, and F. Meseguer, Phys. Rev. B **71**, 125131 (2005).
[55] A. Chutinan and S. John, Phys. Rev. E **71**, 026605 (2005).
[56] J. B. Pendry and A. MacKinnon, Phys. Rev. Lett. **69**, 2772 (1992); P. M. Bell, J. B. Pendry, L. Martin Moreno, and A. J. Ward, Comput. Phys. Commun. **85**, 306 (1995).
[57] D. Cassagne, A. Reynolds, and C. Jouanin, Opt. Quantum Electron. **32**, 923 (2000).
[58] V. Yannopapas, N. Stefanou, and A. Modinos, J. Phys.: Condens. Matter **9**, 10261 (1997).
[59] N. Stefanou, V. Yannopapas, and A. Modinos, Comput. Phys. Commun. **113**, 49 (1998).
[60] V. Yannopapas, N. Stefanou, and A. Modinos, Phys. Rev. Lett. **86**, 4811 (2001).
[61] N. Stefanou, V. Yannopapas, and A. Modinos, Comput. Phys. Commun. **132**, 189 (2000).
[62] P. P. Ewald, Phys. Z. **14**, 465 (1913); Ann. Phys. **54**, 519 (1917); Rev. Mod. Phys. **37**, 46 (1965).
[63] V. Mocella, Opt. Express **13**, 1361 (2005).
[64] S. G. Johnson and J. D. Joannopoulos, Appl. Phys. Lett. **77**, 3490 (2000).
[65] M. Qi, E. Lidorikis, P. T. Rakich, S. G. Johnson, J. D. Joannopoulos, E. P. Ippen, and H. I. Smith, Nature (London) **429**, 538 (2004).
[66] Notice that this symmetry property is preserved when each sphere in the opal structure is replaced with a set of [111]-oriented cylinders.
[67] F. López-Tejeira, T. Ochiai, K. Sakoda, and J. Sánchez-Dehesa, Phys. Rev. B **65**, 195110 (2002).